Cellular/Molecular

Supralinear Ca^{2+} Influx into Dendritic Tufts of Layer 2/3 Neocortical Pyramidal Neurons *In Vitro* and *In Vivo*

Jack Waters, Matthew Larkum, Bert Sakmann, and Fritjof Helmchen
Abteilung Zellphysiologie, Max-Planck-Institut für medizinische Forschung, 69120 Heidelberg, Germany

Pyramidal neurons in layer 2/3 of the neocortex are central to cortical circuitry, but the intrinsic properties of their dendrites are poorly understood. Here we study layer 2/3 apical dendrites in parallel experiments in acute brain slices and in anesthetized rats using whole-cell recordings and Ca^{2+} imaging. We find that backpropagation of action potentials into the dendritic arbor is actively supported by Na^{+} channels both *in vitro* and *in vivo*. Single action potentials evoke substantial Ca^{2+} influx in the apical trunk but little or none in the dendritic tuft. Supralinear Ca^{2+} influx is produced in the tuft, however, when an action potential is paired with synaptic input. This dendritic supralinearity enables layer 2/3 neurons to integrate ascending sensory input from layer 4 and associative input to layer 1.

Key words: **neocortex; dendrite; two-photon; calcium; layer 2/3; backpropagation**

Introduction

Pyramidal neurons, identified by Golgi (1886), are the most abundant cell type in the mammalian cerebral cortex, constituting >70% of rat visual cortical neurons (Zilles, 1990). Many, perhaps most, are in layer 2/3 (L2/3). L2/3 neurons receive sensory input via excitatory synapses onto their basal dendrites from L4 spiny stellate neurons (Lübke et al., 2000; Feldmeyer et al., 2002). In addition, L2/3 neurons extend their apical dendrites into L1. This is the principal input layer for projections from nonspecific thalamic nuclei and higher order sensory areas, which modulate the processing of sensory input in somatosensory and visual cortices (Cauller and Kulics, 1991; Mignard and Malpeli, 1991; Ahissar et al., 2000). Because only L2/3 and L5 pyramidal neurons typically respond to L1 input (Cauller and Connors, 1994), these neurons are probably pivotal elements through which superficial afferents affect neocortical circuitry.

If apical dendrites of L2/3 neurons were passive, EPSPs from synapses in L1 would be substantially attenuated en route to the soma. In neocortical L5 and hippocampal CA1 pyramidal neurons, the effectiveness of distal input is enhanced by dendritic voltage-dependent conductances, which support active backpropagation of axo-somatically initiated action potentials (APs), dendritic Ca^{2+} influx, and dendritic initiation of APs (Yuste and Tank, 1996; Häusser et al., 2000; Reyes, 2001). However, dendritic properties typically are studied in brain slices (*in vitro*). It is unclear whether active properties are as influential under *in vivo* conditions, in which background synaptic and neuromodulatory activity might alter their effectiveness.

L2/3 neurons have received little attention, even *in vitro*, perhaps because their thin dendrites make dendritic recordings particularly challenging; however, their superficial location has encouraged investigation in anesthetized animals using intracellular recording and two-photon Ca^{2+} imaging (Svoboda et al., 1997, 1999). AP amplitudes measured in dendritic impalements showed a pronounced decline with distance from the soma (Svoboda et al., 1999) that has been cited as evidence that active backpropagation is suppressed in cortical pyramidal neurons *in vivo* (Steriade, 2001a,b). Suppression might be consistent with the high rates of spontaneous activity commonly observed *in vivo*, because GABAergic input can inhibit backpropagation *in vitro* (Tsubokawa and Ross, 1996). However, the dendritic properties of L2/3 neurons have not been carefully characterized *in vitro*, making comparison with the *in vivo* situation difficult. Comparison with other cell types (including L5 pyramidal cells) is also difficult, because active phenomena depend on morphology and specific ion channel composition (Vetter et al., 2001; Migliore and Shepherd, 2002).

Here we study the active properties of L2/3 neuron apical dendrites in parallel experiments *in vitro* and *in vivo*, using whole-cell recording and Ca^{2+} imaging. We take advantage of experimental techniques that are feasible only in brain slices, permitting a more detailed explanation of our *in vivo* data. We find that active conductances are present throughout the apical dendrite both *in vitro* and *in vivo*. These conductances support AP backpropagation and give rise to a large dendritic Ca^{2+} signal when a backpropagating AP is paired with distal synaptic input.

Materials and Methods

In vitro *electrophysiology and imaging*. *In vitro* recordings were obtained from primary somatosensory neocortex in parasagittal slices from postnatal day (P) 27–31 Wistar rats. In a few experiments, older animals (up to P46) were used. Because no differences were observed between data gathered at P28 and older ages, all data were pooled. Animals were deeply anesthetized with halothane. After decapitation, the brain was rapidly removed into ice-cold, oxygenated solution containing (in mM): 125 NaCl, 25 $NaHCO_3$, 2.5 KCl, 1.25 NaH_2PO_4, 1 $MgCl_2$, 25 glucose, and 2

Received June 7, 2003; revised July 15, 2003; accepted July 15, 2003.

This work was supported by a Marie Curie individual fellowship from the European Community to J.W. (contract number QLGA-CT-2001-50999). We thank Michael Brecht and Troy Margrie for help with *in vivo* whole-cell recording techniques and Nathan Urban for assistance with the MicroMax camera.

Correspondence should be addressed to Jack Waters, Abteilung Zellphysiologie, Max-Planck-Institut für medizinische Forschung, Jahnstrasse 29, 69120 Heidelberg, Germany. E-mail: jwaters@mpimf-heidelberg.mpg.de.

 0270-6474/03/238558-10$15.00/0

mM $CaCl_2$, pH 7.4. Slices (300 μm thick) were cut with a vibrating microslicer and maintained at 37°C in the above solution for 15–120 min before use. Slices were perfused continuously with the above solution at 35 ± 2°C throughout the experiments. In some experiments (see Figs. 6*b*, 7), GABAergic inputs were partially blocked by adding 2.5 μM bicuculline and 1 μM (2*S*)-3-[[(1*S*)-1-(3,4-dichlorophenyl)ethyl]amino-2-hydroxypropyl](phenylmethyl)phosphinic acid to the perfusate.

L2/3 pyramidal neurons were identified by their position in the slice and by their pyramidal somata. Both L1 and L4 were readily distinguished under bright-field illumination. Whole-cell recordings from somata and from dendrites were obtained with the aid of infrared differential interference contrast optics. Somatic (4–6 MΩ) and dendritic (10–20 MΩ) recording pipettes were filled with an intracellular solution containing (in mM): 135 K gluconate, 4 KCl, 10 HEPES, 10 Na_2-phosphocreatine, 4 Mg-ATP, 0.3 Na-GTP, 0.2% biocytin, pH 7.2; 291–293 mOsm. For dendritic recordings, 10 μM Alexa 568 (Molecular Probes, Eugene, OR) was included in the somatic pipette so that the apical dendrite could be located with the aid of a camera after a whole-cell recording was established at the soma.

Electrical recordings were obtained using Axoclamp-2B amplifiers (Axon Instruments, Union City, CA). AP amplitudes were measured from resting membrane potential to peak. Half-widths were measured at half-height, meaning half the voltage difference between the start of the AP upstroke (threshold) and its peak. Latencies between responses at somatic and dendritic pipettes were measured as the temporal difference between the half-amplitudes of responses at the two locations.

For Ca^{2+} imaging experiments *in vitro*, 100 μM Oregon green BAPTA-1 was added to the intracellular solution unless noted otherwise. Neurons were typically allowed to fill with dye for 20–30 min before imaging. *In vitro* Ca^{2+} imaging was performed using a 40× water immersion objective [numerical aperture (NA) 0.8; Zeiss] and a frame-transfer charge-coupled device camera (PXL or MicroMax, Roper Scientific, Tucson, AZ). The specimen was illuminated during data collection with 490 nm light from a monochromator (TILL Photonics, Munich, Germany). Emitted fluorescence was detected through a 496 nm long-pass dichroic mirror and a 515 nm long-pass emission filter.

Both dendritic and background signals were collected after centering a 5 × 7 grid of rectangular regions of interest over part of the apical dendrite (each region ~5–10 × 5–10 μm). On-chip binning was used for each region of interest. Data were thus obtained simultaneously from several neighboring regions, enabling the most appropriate background regions to be selected off-line. This minimized the effects of uneven illumination intensity and of fluorescence signals from out-of-focus structures. Fluorescence intensities were sampled at 40 Hz. Fluorescence transients were measured at different distances from the soma in semi-random order, rather than in sequence proceeding away from the soma. In addition, recordings were often sufficiently prolonged to allow the Ca^{2+} measurements to be repeated at several different points in time. We therefore were able to verify that dendritic properties were not changing throughout the experiment. Ca^{2+} signals were expressed as fluorescence changes after subtraction of the background trace and division by the resting fluorescence ($\%\Delta F/F$) (Helmchen, 2000).

In experiments in which large parts of the dendritic tree were imaged simultaneously, a low-magnification objective was used (20× water immersion, NA 0.5; Olympus). We used 10 × 10 on-chip binning, and data were acquired as full-frame images at 25 Hz.

Calcium profiles (see Results) were generated from both low- and high-resolution data sets. For comparison of data from different cells, data derived from a single neuron were normalized in both dimensions. First, the distance along the apical dendrite was normalized to the soma–pia distance to facilitate comparison of cells located at different depths from the pial surface. The soma–pia distance was defined as the length of a straight line drawn from the soma along the apical dendritic trunk to the pial surface. The amplitudes of the calcium transients were subsequently normalized to the maximum amplitude observed in that neuron. To minimize the effects of measurement noise, the data from an individual cell were fit with a skewed Gaussian function (see Fig. 2*f*, inset), and the maximum amplitude was defined as the maximum value of the fit.

For tetrodotoxin (TTX) experiments involving two-electrode voltage clamp, one somatic electrode was initially used for voltage recording and the other was used to inject brief current pulses to induce single APs (see Fig. 3*b*). After 2 μM TTX was added to the perfusing solution, the action potential was eliminated. The neuron was then voltage clamped at the soma using a two-electrode voltage-clamp circuit (gain 3–150 V/V). Using the AP waveform recorded before TTX application as voltage command, AP-like waveforms were imposed at the soma. The similarity of command and acquired voltage traces indicated that voltage control at the soma was very good.

After recording, the slice was fixed for 2 d at 4°C in 4% paraformaldehyde in phosphate buffer (75 mM Na_2HPO_4 and 25 mM NaH_2PO_4, pH 7.2). Intracellular biocytin was visualized using the avidin–biotin horseradish peroxidase reaction and 3,3-diaminobenzidine as described previously (Lübke et al., 2000). Neurons were reconstructed using Neurolucida software (MicroBrightField, Colchester, VT).

In vivo *electrophysiology and imaging.* P27–31 Wistar rats were anesthetized with urethane (1–2 gm/kg). Depth of anesthesia was sufficient to eliminate pinch withdrawal, corneal reflex, and vibrissal movements. A small (2 × 2 mm) craniotomy was opened over the barrel cortex, and the dura was removed (coordinates for center of craniotomy: 2 mm posterior to bregma, 5–6 mm lateral) (Chapin and Lin, 1990). The craniotomy was covered with agar (1–1.5%, type III-A, Sigma, St. Louis, MO) in the following solution (in mM): 135 NaCl, 5.4 KCl, 1 $MgCl_2$, 1.8 $CaCl_2$, 5 HEPES. A glass coverslip was positioned over the agar. Gentle downward pressure was applied to the coverslip throughout the experiment. This reduced motion of the cortex during recording and imaging.

Whole-cell patch-clamp recordings were obtained using a "blind" technique as described previously (Margrie et al., 2002). Pipettes (4–6 MΩ) were filled with the same intracellular solution as used in slice experiments. A higher dye concentration [200 μM Oregon Green BAPTA (OGB)-1)] was used to compensate for the higher access resistances typically encountered *in vivo*. Positive pressure (200–300 mbar) was applied to the pipette as it was inserted through the agar and L1 of the cortex. The positive pressure was reduced to 25–30 mbar when the tip was at approximately the upper limit of L2/3. The pipette was then advanced in 2 μm steps through L2/3. Voltage pulses were applied to the pipette (10 mV, 30 msec, 10 Hz), and the current response was monitored. Positive pressure was relieved when the series resistance of the electrode abruptly increased immediately after a 2 μm step, indicating that the tip of the pipette may have been pushed against a neuronal plasma membrane. Gentle suction (up to 100 mbar) was applied where necessary to obtain a gigaohm seal. Initial access resistance in the whole-cell configuration was typically 30–60 MΩ at the soma or 40–80 MΩ in the dendrite.

L2/3 pyramidal neurons were identified by (1) their regular firing pattern, (2) their characteristic apical dendrite and distal tuft, and (3) the depth of the soma below the pia (150–500 μm) measured using the two-photon microscope. Every neuron responded to whisker stimulation (air-puff) with a 5–15 mV EPSP, confirming that all recordings were obtained from barrel cortex. The soma was located by focusing down into the brain from the pial surface using the fluorescent image of the dye-filled electrode as a guide. Whole-cell recordings including calcium imaging *in vivo* typically lasted ~1 hr, although neurons were often visible after filling with indicator dye for 10–15 min. Dendritic recordings were obtained with the same methodology. The distance of the recording site from the soma (up to 150 μm) was measured during the experiment using the two-photon microscope.

In vivo Ca^{2+} imaging was combined with whole-cell recording as described previously (Helmchen and Waters, 2002). Two-photon microscopy was performed using a custom-built microscope (Svoboda et al., 1997). The specimen was illuminated with 840 nm light from a pulsed Ti:sapphire laser with a repetition rate of 80 MHz and 100–150 fsec pulse width (Mira 900; Coherent, Santa Clara, CA). Excitation light was focused onto the specimen using a 40×, NA 0.8 water immersion objective (Zeiss). Emitted light was collected in the epifluorescence configuration through a 680 nm long-pass dichroic mirror and an infrared-blocking emission filter (Schott BG39) using a photomultiplier tube (Hamamatsu). Scanning and image acquisition were controlled using custom software (R. Stepnoski and M. Müller, Lucent Technologies, NJ; and MPImF, Heidelberg, Germany).

Ca^{2+} transients were measured using 64-pixel line scans at 500 Hz. Fluorescence was averaged over the width of the dendrite and expressed as relative fluorescence changes ($\%\Delta F/F$) after subtraction of background fluorescence from a neighboring region. Traces were filtered in the temporal domain using a three- to five-point Gaussian filter. Peak amplitudes were determined from averages of several trials by fitting the decaying phase of the Ca^{2+} transient with a single exponential. The amplitude was then estimated by back-extrapolating the fit to the time point corresponding to the start of the rising phase of the response. Calcium profiles were fit with a skewed Gaussian curve using the equation $y = a(x - c)^b \exp(-(x - c)^2/d^2)$, where *a, b, c,* and *d* are fitting parameters.

All experimental procedures were performed in accordance with the animal welfare guidelines of the Max Planck Society.

Results

Action potential recordings from apical dendrites

The spread of APs into L2/3 pyramidal cell dendrites was characterized both *in vitro* and *in vivo* using dendritic whole-cell recordings. In brain slices, simultaneous recordings were obtained from the soma and apical dendrite of L2/3 pyramidal neurons (Fig. 1*a*). Dendritic recording sites were proximal to the primary bifurcation and up to 320 μm from the soma. In anesthetized rats, recordings were obtained from either the soma or the proximal apical dendrite (up to 150 μm from the soma) (Fig. 1*b*). *In vivo*, the membrane potential fluctuated between a resting ("down") and a depolarized ("up") state. Resting membrane potential, input resistance, AP amplitude from rest, and AP half-width, measured at the soma, were similar *in vitro* and *in vivo* [V_m −78 ± 1.3 mV *in vitro* ($n = 15$) and −74 ± 2 mV *in vivo* ($n = 15$; measured in the down state); R_N 47 ± 4.8 MΩ *in vitro* ($n = 16$; range, 23–86 MΩ) and 45 ± 3.6 MΩ *in vivo* ($n = 16$; range, 22–73 MΩ; down state); AP amplitude 119 ± 1.7 mV *in vitro* ($n = 27$) and 116 ± 1.7 mV *in vivo* ($n = 16$ with access resistance <35 MΩ); AP half-width 0.83 ± 0.02 msec *in vitro* ($n = 27$) and 0.78 ± 0.02 msec *in vivo* ($n = 16$)].

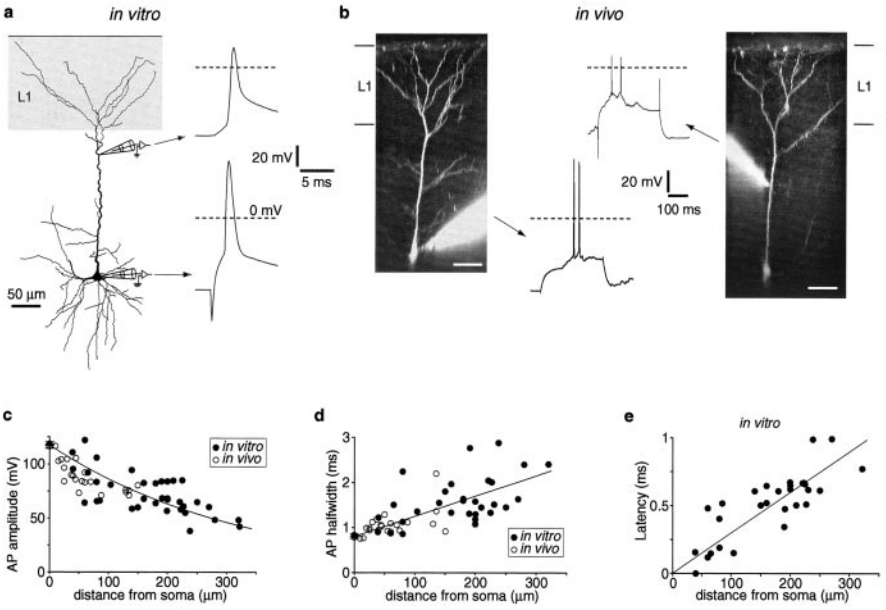

Figure 1. Dendritic recordings of backpropagating APs. *a*, Dual recording from soma and dendrite of an L2/3 pyramidal neuron in a slice preparation. Left, Biocytin reconstruction with recording locations indicated schematically (dendritic pipette was 225 μm from the soma). Shaded region represents approximate position of L1. Right, Simultaneous somatic and dendritic recordings of an AP induced by somatic current injection (2 msec pulse; 2 nA). *b*, Somatic and dendritic AP recordings *in vivo*. Images are side projections of stacks of two-photon fluorescence images (same scale as in *a*). Left, Somatic recording from an L2/3 pyramidal neuron filled with OGB-1. Somatic APs evoked by a 300 msec current injection (300 pA) are shown in the bottom trace. Right, Dendritic recording from a different neuron. The dendritic recording pipette was located 150 μm from the soma. APs evoked by a 300 msec current injection (700 pA) are shown in the top trace. *c*, Amplitudes of single APs evoked by current injection *in vitro* (filled symbols) and *in vivo* (open symbols) as a function of distance from the soma. Each point represents a single dendritic recording, with one recording per neuron. Somata were located 300–505 μm from the pia *in vitro* and 210–570 μm *in vivo*. Amplitudes were measured from resting membrane potential. An exponential decay was fit through all data points (solid line; $\tau = 317$ μm; asymptote constrained to zero). *d*, AP half-widths determined *in vitro* (filled symbols) and *in vivo* (open symbols) plotted as a function of distance from the soma. Half-width was determined as the width at half-height from the inflection point to the peak of the AP. A linear fit to all data points yielded a slope of 4.5 μsec/μm (constrained to 0.8 msec at soma). *e*, Latencies of dendritic relative to somatic responses measured at half-heights of APs *in vitro*. A linear fit through the origin yielded a propagation velocity of 330 μm/msec.

Along the apical dendritic trunk, APs decreased in amplitude and broadened (Fig. 1*c*,*d*). Attenuation and broadening were similar *in vitro* and *in vivo* with amplitudes ~75 mV at 150 μm from the soma (distance constant, 317 μm). From the dual recordings obtained *in vitro*, the propagation velocity was found to be 330 μm/msec (Fig. 1*e*).

Note that for the data shown in Figure 1, APs were evoked by somatic current injection *in vitro*. With only one recording electrode *in vivo*, APs were necessarily evoked by dendritic current injection. Control experiments *in vitro* indicated that this comparison is valid. First, up to 150 μm from the soma, current injection into the dendrite led to somatic AP initiation (data not shown). Furthermore, dendritic amplitudes of APs evoked by dendritic current injections (80–190 μm from the soma) were only 5.8 ± 2.6% larger ($n = 8$) than those of APs evoked by somatic current injection. Hence measured action potential amplitudes were independent of the location of current injection (up to 150 μm from the soma). In addition, the similarity of dendritic AP amplitudes *in vitro* and *in vivo* was not dependent on bridge balance because they were also similar when measured from threshold (*in vitro*: 38 ± 2.5 mV, $n = 7$, 140–190 μm from the soma; *in vivo*: 41.7 ± 0.35 mV, $n = 4$, 130–135 μm from the soma).

We conclude that an AP is attenuated and broadened as it travels in the retrograde direction along the apical dendrite of a L2/3 neuron. The amount of attenuation and broadening is similar in brain slices and in anesthetized rats.

AP-evoked dendritic Ca^{2+} transients are similar *in vitro* and *in vivo*

We next compared the spatial pattern of dendritic Ca^{2+} influx evoked by single APs *in vitro* and *in vivo*. Neurons were filled with the Ca^{2+} indicator OGB-1 via somatic recording pipettes. Fluorescence was measured with a CCD camera in brain slice experiments and using two-photon microscopy in anesthetized rats. In the proximal apical trunk, single APs evoked relative fluorescence changes of 30–105%. Mean peak amplitudes were 84 ± 6.8% *in vitro* ($n = 11$) and 50 ± 4% *in vivo* ($n = 13$), and decay time constants were 180 ± 18 msec *in vitro* ($n = 13$) and 168 ± 18 msec *in vivo* ($n = 13$). Note that the pipette indicator concentration for *in vivo* recordings was twice that used *in vitro* to compen-

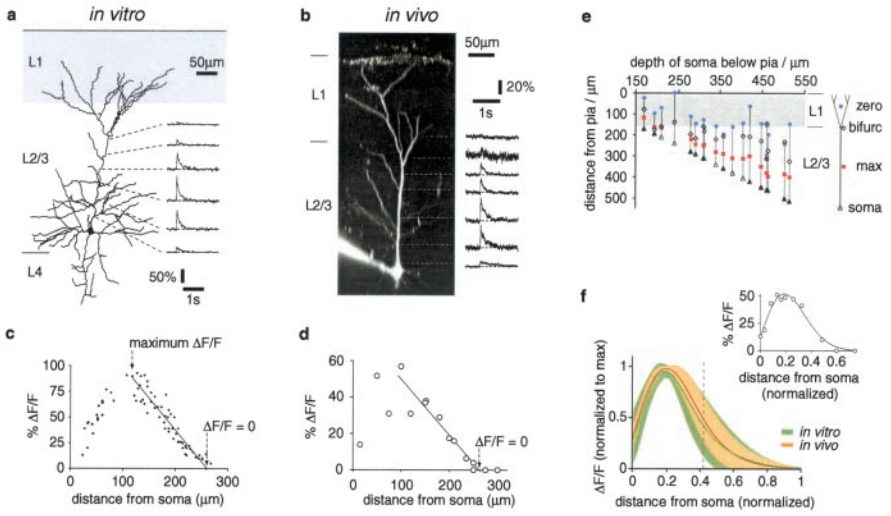

Figure 2. Single APs evoke similar dendritic Ca^{2+} profiles *in vitro* and *in vivo*. *a*, *b*, Examples of Ca^{2+} transients in apical dendrites, each evoked by a single somatic AP. Biocytin reconstruction of an L2/3 neuron studied *in vitro* (*a*; 500 μm from the pia). Two-photon side projection of a L2/3 neuron studied *in vivo* (*b*; 400 μm from the pia). APs were initiated by 3–5 msec somatic current injections. Traces are averages of 5–20 (*a*) or 3–5 trials (*b*). *c*, *d*, Spatial profile of peak Ca^{2+} transients in the apical dendrites of the cells shown in *a* and *b*, respectively. The dendritic location distal to which no Ca^{2+} transient was detectable ($\Delta F/F = 0$) was estimated from a linear fit to the declining portion of the profile. *e*, Schematic representation of Ca^{2+} profiles evoked by single APs for neurons recorded *in vitro* (filled soma symbols) and *in vivo* (open soma symbols). The neurons are ranked according to the depth of their somata below the pia. Each neuron is represented as a vertical column of four points (connected by a vertical line). These points represent the location of the soma (triangle), the principal bifurcation (open diamond), the maximum peak amplitude of Ca^{2+} transient (red square), and the point at which the peak amplitude of the Ca^{2+} transient declined to zero (blue circle; $\Delta F/F = 0$) as illustrated on the schematic neuron to the right. All data are from somatic recordings. *f*, Normalized Ca^{2+} profiles for *in vitro* and *in vivo* recordings. The profile for each neuron was normalized to the distance between soma and pia and fit with a skewed Gaussian curve (see Materials and Methods). The profile was subsequently normalized to its maximum value (inset shows an example from an *in vivo* experiment). Normalized profiles were averaged for *in vitro* (green; $n = 9$) and *in vivo* (orange/yellow; $n = 7$) experiments. Shaded areas represent $\pm$ 1 SD from the mean. Dashed line represents mean position of principal bifurcation (0.41 $\pm$ 0.05 *in vitro* and 0.43 $\pm$ 0.03 *in vivo*). All data are from somatic recordings.

sate for the higher access resistances usually encountered *in vivo*. A possible explanation for the smaller amplitudes *in vivo* is that the extracellular Ca^{2+} concentration may have been lower than the 2 mM used in slice experiments.

In 20 neurons (13 *in vitro*, 7 *in vivo*) spatial profiles of Ca^{2+} transient amplitudes ("Ca^{2+} profiles") were obtained using sequential measurements from different locations along the apical dendrite (Fig. 2*a–d*). In all cases the amplitude of the Ca^{2+} transient increased with distance from the soma, reaching a maximum value in the proximal apical dendrite and then declining to undetectable levels more distally. No substantial steps were observed in the distal decline in any neuron, suggesting that AP spread was not abruptly altered at dendritic branch points. Furthermore, there were no "Ca^{2+} hotspots" of the type reported in bitufted neurons (Kaiser et al., 2001).

To determine whether there was a consistent pattern in the heterogeneous group of L2/3 neurons, we displayed data from all neurons on a single plot, representing each cell by the following four locations (Fig. 2*e*): soma, principal bifurcation, location of the maximum of the Ca^{2+} profile, and dendritic position beyond which no Ca^{2+} influx was observed (estimated using a linear fit through the data points distal to the peak of the profile) (Fig. 2*c*,*d*). Two general features of the dendritic Ca^{2+} dynamics are evident from this summary plot. First, the maximum amplitude always occurred in the proximal dendrite between the soma and the principal bifurcation (except in one case, a neuron close to L1 with a bifurcation very close to the soma.) Second, Ca^{2+} signals were always detectable as far as the principal bifurcation.

The most distal location to which Ca^{2+} transients could be observed showed some dependence on somatic depth. In superficial neurons with somata close to the border of L1, single somatic APs evoked Ca^{2+} influx throughout much of L1, although Ca^{2+} transients declined to zero in the very distal, subpial tuft branches in most neurons. In contrast, Ca^{2+} influx was typically visible up to the L1 border but not more distally in deeper neurons (those with somata near the center of L2/3 or close to the border with L4). A likely explanation for this finding is that the distal Ca^{2+} influx depends on the amplitude of the backpropagating AP that remains in distal tuft branches and that this amplitude is smaller in neurons with longer dendrites because of attenuation along the apical trunk. We saw no obvious correlation between dendritic branching pattern and the dendritic location beyond which no calcium transient was observed.

For further comparison of *in vitro* and *in vivo* profiles, we normalized the profile from each neuron to the length of its apical dendrite and to its maximum Ca^{2+} response. We then pooled cells into *in vitro* and *in vivo* data sets (Fig. 2*f*) (see Materials and Methods for a description of the normalization procedure). The normalized profiles were remarkably similar under *in vitro* and *in vivo* conditions with the maximum Ca^{2+} response at ~20% of the distance from soma to pia. Likewise, in both conditions the amplitude of the Ca^{2+} transient declined to 10% of its maximum value at ~65% of the distance from soma to pia. At this distance we estimate the average AP amplitude to be ~50 mV, on the basis of a fitted curve through a version of Figure 1*c* normalized for soma–pial distance.

Therefore, L2/3 neurons with different somatic locations (and hence different lengths of apical trunk) share similar dendritic Ca^{2+} profiles. Furthermore, neurons examined in the anesthetized animal and in the slice preparation displayed remarkably similar profiles.

Action potential backpropagation is active

The data presented above show that action potentials spread a substantial distance into the apical dendrites of L2/3 neurons, resulting in Ca^{2+} entry throughout much of the dendritic tree. Although backpropagation is decremental, the attenuation of AP amplitude is less than expected for purely passive spread along the dendrite. Furthermore, this attenuation is comparable with that in L5 neurons, in which backpropagation is actively assisted by dendritic Na^+ channels (Stuart and Sakmann, 1994; Larkum et al., 2001; Stuart and Häusser, 2001). Our data therefore suggest that AP backpropagation in L2/3 pyramidal cell dendrites is actively supported by dendritic Na^+ channels.

To demonstrate this directly, we examined dendritic potentials *in vitro* before and after blocking Na^+ channels with TTX. Three whole-cell recordings were established simultaneously, two at the soma and one on the apical dendrite (Fig. 3*a*). Initially, AP amplitudes at the soma and the dendrite were recorded under

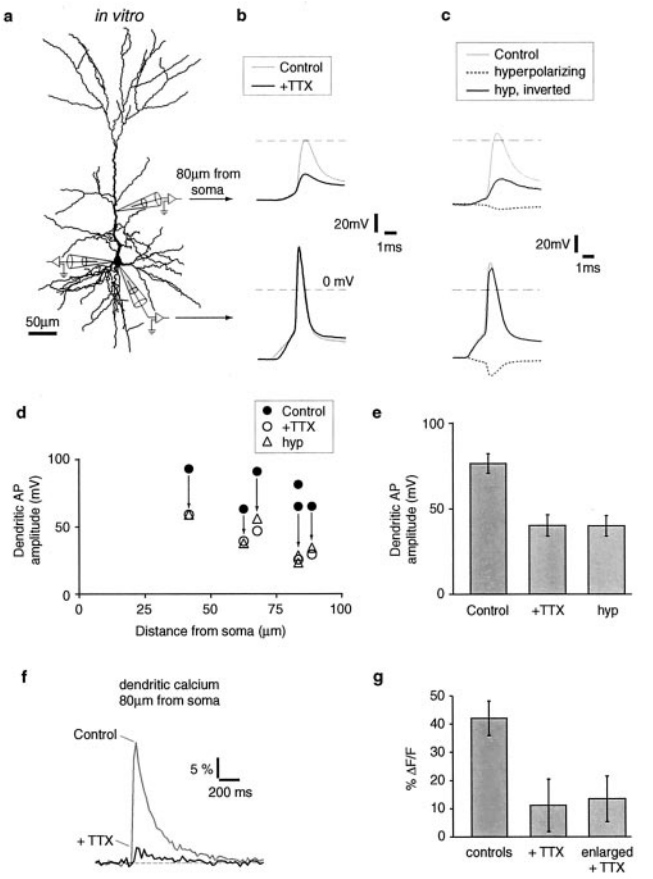

Figure 3. AP backpropagation and Ca^{2+} influx require Na^+ channels. *a*, Triple whole-cell recording from a slice preparation. The positions of the recordings are shown schematically on the biocytin reconstruction. *b*, Somatic and dendritic recordings during an AP induced by somatic current injection through the third (somatic) electrode (bridge balance mode; gray traces) and during somatic injection of a similar waveform using two-electrode voltage clamp in 2 μM TTX (black traces). *c*, Somatic (bottom) and dendritic (top) recordings from another L2/3 neuron showing passive spread of hyperpolarizing waveforms (dendritic pipette 80 μm from the soma). Gray traces, AP evoked by somatic current injection (bridge balance mode, no TTX). Dashed traces, Responses to somatic injection of a scaled-down, hyperpolarizing AP-like waveform (two-electrode voltage clamp, no TTX; 30% of original amplitude). Black traces, Hyperpolarizing response reinverted and rescaled for comparison with the original AP. *d*, Reduction of dendritic AP amplitude as a function of distance from the soma ($n = 6$ experiments). Filled circles represent original AP amplitudes. Open circles represent amplitude of response to depolarizing AP-like waveforms in TTX. Triangles represent reinverted scaled responses to hyperpolarizing AP waveforms (no TTX). *e*, Summary plot for the six neurons shown in *d*. Bars represent mean (±SEM). Both TTX and hyperpolarization groups were significantly different from control ($p < 0.01$; paired *t* test). *f*, Ca^{2+} transients recorded from a proximal apical dendrite evoked by an AP (gray trace; 30% $\Delta F/F$) and AP-like waveform in TTX under two-electrode voltage clamp (black trace; 4% $\Delta F/F$). Peak voltages at the soma were +36 mV for the original AP and +30 mV in TTX. Half-widths were 1.13 msec for control and 1.03 msec in TTX. *g*, Pooled data from three neurons, showing mean (±SEM) amplitude of the Ca^{2+} transient under control conditions, after TTX application, and using the enlarged AP waveform as command. Somatic positions were 330, 420, and 425 μm from the pia. Dendritic regions of interest were 80, 140, and 70 μm from the soma, respectively. Both TTX and hyperpolarization groups were significantly different from control ($p < 0.06$; paired *t* test).

current clamp. After blocking Na^+ channels with 2 μM TTX, the somatic AP waveform recorded before TTX application was imposed on the soma using two-electrode voltage clamp. The somatic peak amplitude of the AP-like waveform imposed under voltage clamp was similar to that of the recorded AP (control 121 mV; in TTX 120 mV), indicating that the soma was adequately voltage clamped. In contrast, the dendritic depolarization was strongly attenuated, even close to the soma (peak amplitudes of 65 mV in control and 26 mV in TTX; 80 μm from the soma) (Fig. 3*b*).

These data suggest that AP backpropagation is actively supported by dendritic Na^+ channels and that TTX converted the active dendrite into a dendrite that acts more like a passive cable. We confirmed this by injecting hyperpolarizing AP waveforms at the soma in the absence of TTX (Fig. 3*c*). AP waveforms with 30% of the control amplitude and of reversed polarity were attenuated as strongly as the depolarizing AP waveforms in TTX. This was observed in six experiments with dendritic recordings 40–90 μm from the soma in neurons with somata 300–470 μm from the pial surface of the slice (Fig. 3*d*,*e*). We conclude that AP backpropagation in apical dendrites of L2/3 pyramidal neurons is dependent on activation of Na^+ channels.

Dendritic Ca^{2+} signals were also dependent on Na^+ channels because proximal Ca^{2+} influx was greatly reduced by application of TTX (Fig. 3*f*) (control amplitude 30% $\Delta F/F$; in TTX 4% $\Delta F/F$). Even using a 1.5-fold enlarged AP waveform as voltage command (peak voltage + 60 mV; half-width 1.13 msec; data not shown), the Ca^{2+} signal was far smaller than that evoked before TTX application (6% $\Delta F/F$ in TTX). Again the recorded AP waveform under two-electrode voltage clamp was very similar to the control AP (Fig. 3*b*). Furthermore, prolonged voltage steps produced large dendritic Ca^{2+} transients, showing that dendritic Ca^{2+} channels were still functional (data not shown; 200 msec steps to −40, −20, and 0 mV resulted in Ca^{2+} transient amplitudes of 26, 28, and 50%, respectively). Similar reductions of Ca^{2+} influx were observed in three neurons. On average, Ca^{2+} transients were reduced by 76 ± 18 and 70 ± 15% for original and enlarged AP waveforms, respectively (Fig. 3*g*).

In summary, both backpropagation of single APs and the resulting Ca^{2+} influx into apical dendrites of L2/3 pyramidal neurons *in vitro* depend on dendritic Na^+ channels. In view of the striking similarity of AP attenuation and Ca^{2+} profiles derived from *in vitro* and *in vivo* experiments, it is very likely that this conclusion also applies to L2/3 neurons *in vivo*.

Excitability of distal tuft branches

The above experiments demonstrate that APs backpropagate actively but are nonetheless attenuated as they spread along the apical trunk of deep L2/3 neurons. The lack of a Ca^{2+} signal in tuft branches therefore could result from either the absence of Ca^{2+} channels or insufficient depolarization in the distal dendrite. To distinguish between these two possibilities, we measured dendritic tuft Ca^{2+} transients evoked by bursts of APs.

In vitro we imaged Ca^{2+} influx in the tips of dendritic branches 40–100 μm from the pial surface of the slice (Fig. 4*a*). Brief bursts of only two to three APs were sufficient to produce small Ca^{2+} transients, and four to five APs evoked much larger signals (Fig. 4*b*). These transients were observed with high-frequency (150 Hz) bursts, whereas lower-frequency (50 Hz) trains of four to five APs produced little or no Ca^{2+} signal. This supralinear increase in the amplitude of the Ca^{2+} transient with increasing numbers of APs was observed in five neurons (Fig. 4*c*).

In addition, we monitored the spatial profile of Ca^{2+} influx in proximal and distal dendrites simultaneously at low magnification (20× objective) (Fig. 4*d*). Throughout the dendritic tree the amplitudes of Ca^{2+} transients became larger with increasing numbers of APs (Fig. 4*e*). Calculating the percentage fluorescence change per AP indicated that, as in the previous experiments (Fig. 4*a–c*), summation was supralinear in distal dendrites. In addition, these profiles revealed that the supralinearity was limited to the distal region because linear summation was ob-

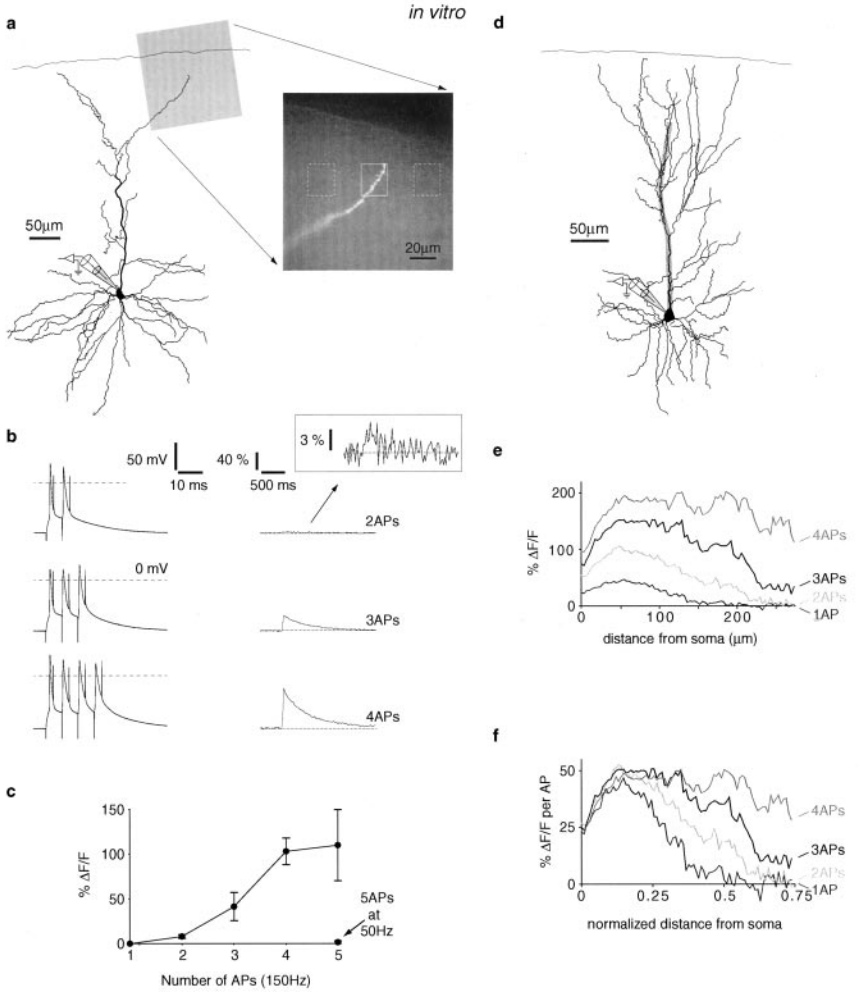

Figure 4. AP bursts evoke Ca^{2+} signals in tuft branches *in vitro*. *a*, Biocytin fill of a L2/3 neuron (soma 395 μm below the pia). Enlarged fluorescence image shows a terminal branch filled with OGB-1. A 500 μM concentration of OGB-1 was used in these experiments to facilitate dendritic filling. Solid white box represents region of interest, centered 40 μm below pia; dashed white boxes represent flanking background regions. *b*, Ca^{2+} transients in the dendrite shown in *a* in response to two to four APs evoked by somatic current injections at 150 Hz: peak $\Delta F/F$, 2APs 5%; 3APs 44%; 4APs 115%. *c*, Pooled data from five neurons *in vitro* with somata 300–470 μm from the pia. Four neurons displayed Ca^{2+} signals to 2 APs (4–17% $\Delta F/F$). All five neurons responded to 3 APs (12–67% $\Delta F/F$). In only one neuron, 5 APs at 50 Hz evoked a Ca^{2+} signal that was very small (<5% $\Delta F/F$). *d*, Biocytin fill of another neuron (soma 350 μm from the pia). The Ca^{2+} profiles were analyzed along the gray line. *e*, Spatial Ca^{2+} profiles derived from low-magnification images, showing the peak amplitudes of Ca^{2+} transients induced by 1–4 APs (at 150 Hz) at different spatial locations along the gray line shown in *d*. *f*, The same data as in *e* represented as fluorescence change per action potential. Each profile was divided by the number of APs in the burst. The abscissa was normalized to the distance between soma and pia.

served in more proximal regions (Fig. 4*f*). Similar data were obtained in three cells (data not shown).

Supralinear summation also occurred with high-frequency bursts of APs *in vivo* ($n = 6$ cells) (Fig. 5*a*,*b*). These data were typically collected from more proximal regions of the tuft branches than in the equivalent slice experiments (range, 10–175 μm from the pia). In several additional experiments, we were able to obtain *in vivo* measurements from subpial dendritic tips (Fig. 5*c*). In these terminal branches, Ca^{2+} transients were sometimes observed after high-frequency bursts of four to five APs in five of seven cells (Fig. 5*d*). The amplitudes of these transients were variable, perhaps because of background synaptic activity. We conclude that Ca^{2+} channels are present throughout the apical tuft, including subpial tips in superficial L1, and that these channels may be activated by bursts of APs both *in vitro* and *in vivo*.

Pairing of AP and EPSP evokes supralinear Ca^{2+} influx

Under what conditions might synaptic input contribute to activation of voltage-sensitive channels in the distal dendrite? Distal activation may be particularly likely when synaptic input is paired with a backpropagating AP. For example, supralinear summation of AP and EPSP has been observed in the dendrites of L5 pyramidal neurons (Larkum et al., 1999a; Stuart and Häusser, 2001). We therefore examined the consequences of pairing a single backpropagating AP with EPSPs or EPSP-like depolarization of the apical dendrite *in vitro*.

First, we used dual somatic and dendritic recordings to pair a backpropagating AP with EPSP-like depolarization in the dendrite [artificial EPSP (aEPSP)]. The dendritic electrode was placed near the principal bifurcation and Ca^{2+} transients were monitored in the same region. Figure 6*a* shows electrophysiological recordings and dendritic Ca^{2+} measurements from a single neuron. A somatic AP and an aEPSP, delivered separately, both gave small Ca^{2+} signals (peak $\Delta F/F$ of 7 and 8%, respectively); however, when these two stimuli were paired, with the AP 10 msec before the aEPSP, the amplitude of the dendritic Ca^{2+} transient was greatly increased (peak $\Delta F/F$ 179%). In addition, a second AP occurred 10 msec after the first AP. The large Ca^{2+} influx, however, was not caused by the additional AP because two somatically induced APs at the same frequency (with no aEPSP) were insufficient to produce a comparable influx.

Similar results were obtained in all five neurons examined (Fig. 6*b*). In all cases, pairing evoked a large Ca^{2+} transient near the bifurcation. A second AP was induced in four of these five neurons, although pairing did not result in bursts of multiple APs as reported for L5 neurons (Larkum et al., 1999a, 2001). No second AP occurred in the remaining neuron, but a large Ca^{2+} transient was observed.

Pairing a backpropagating AP with synaptic input evoked by extracellular stimulation in L1 also produced a large distal Ca^{2+} transient. In the example shown in Figure 6*c*, Ca^{2+} transients were measured 175 μm from the soma (near the bifurcation) where a backpropagating AP alone produced very little Ca^{2+} influx (peak $\Delta F/F$ of 10%). No Ca^{2+} influx was observed after an EPSP (peak amplitude at the soma: 18 mV); however, a large Ca^{2+} transient was observed when these two inputs were paired (peak $\Delta F/F$ of 62%). To observe this pairing effect it was necessary to partially block GABA receptors, as in L5 neurons (Larkum et al., 1999a). Summary data from seven neurons are presented in Figure 6*d*. In all cases, pairing evoked a large Ca^{2+} transient near the bifurcation. A second AP was induced in only one neuron, although stronger extracellular stimuli could evoke a second AP (data not shown).

Supralinear distal Ca^{2+} influx was further demonstrated in

measurements of spatial Ca^{2+} profiles at low magnification (Fig. 7). Single AP-evoked Ca^{2+} profiles were similar to those measured at high magnification, showing no Ca^{2+} influx in distal parts of the dendrites (compare Fig. 2*f*). Pairing an AP with a distally evoked EPSP caused additional Ca^{2+} entry near the bifurcation, substantially changing the shape of the Ca^{2+} profile (Fig. 7*a*). In four pairing experiments, supralinear Ca^{2+} influx was observed around the bifurcation, from ~0.3 to 0.7 of the normalized soma–pia distance (Fig. 7*b*,*c*). Subthreshold EPSPs alone caused small Ca^{2+} transients limited to the far distal region.

In summary, interaction of a back-propagating AP with distal synaptic input extends the spatial profile of Ca^{2+} influx, producing a supralinear Ca^{2+} transient in the distal part of the apical trunk and the more proximal part of the tuft.

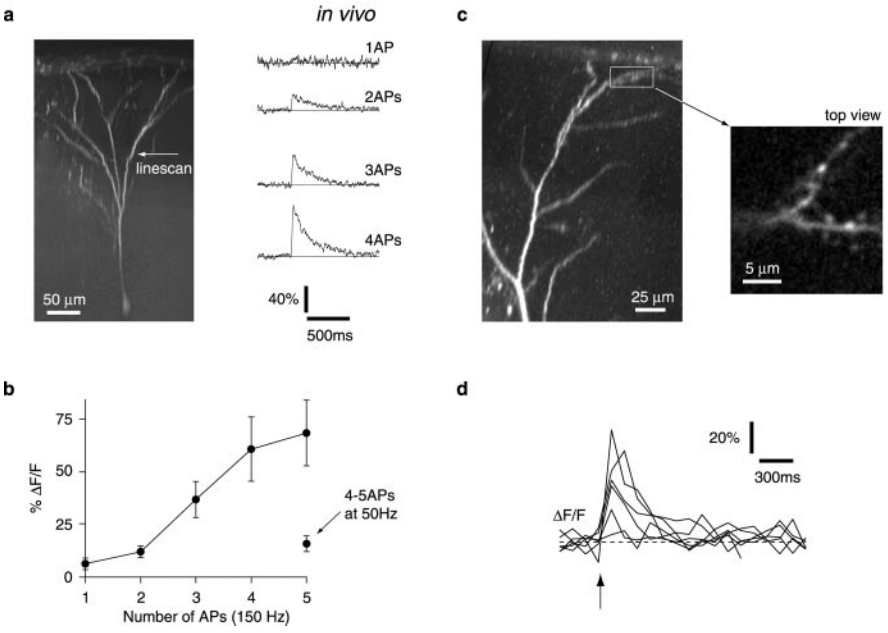

Figure 5. AP bursts evoke Ca^{2+} signals in distal dendrites *in vivo*. *a*, Two-photon side projection of a L2/3 neuron and dendritic Ca^{2+} transients (location marked) evoked by different numbers of APs at 150 Hz. A 500 μM concentration of OGB-1 was used to facilitate dendritic filling. Scale bar, 50 μm. Peak $\Delta F/F$: 1AP 8%; 2APs 20%; 3APs 58%; 4APs 94%. *b*, Pooled data from six neurons *in vivo* with somata 200–365 μm from the pia. Four neurons displayed small Ca^{2+} signals evoked by 1 AP. Both the remaining neurons responded to 2 APs at 150 Hz. *c*, Two-photon side projection of tuft branches of a different neuron (left; 200 μM OGB-1) and top view of the terminal branches (white box; 20 μm below pia). Soma was 350 μm below pia. *d*, Six example fluorescence traces recorded from the terminal branches in *c* in response to 4–5 APs at 150 Hz (arrows). Image series, rather than line scans, were acquired (at 8 Hz). Traces represent background-corrected spatially averaged signals. Note that not every burst evokes a signal.

Discussion

We have studied apical dendrites of L2/3 neocortical pyramidal neurons, in parallel *in vitro* and *in vivo* experiments. This novel approach allowed us to take advantage of techniques feasible only in the cortical slice preparation and to verify the validity of the results in the cortex of the intact animal. We find that AP backpropagation into the apical dendrite is active, resulting in a similar spatial distribution of Ca^{2+} influx *in vitro* and *in vivo*. Although single APs cause minimal Ca^{2+} influx in the dendritic tuft, pairing an AP with synaptic input leads to substantial Ca^{2+} influx in this region of the neuron. These properties may profoundly shape synaptic integration in L2/3 neurons, enhancing the effectiveness of projections to L1 of the neocortex.

Active AP backpropagation in L2/3 neurons

AP amplitudes showed a modest decline with distance from the soma both *in vitro* and *in vivo*. The much stronger decline after block of Na^+ channels *in vitro* indicated that backpropagating APs are actively boosted by these channels. In view of the similarity of AP amplitudes and of Ca^{2+} profiles *in vitro* and *in vivo*, we conclude that backpropagation is also active *in vivo*. This underscores the value of parallel *in vitro* and *in vivo* experiments.

The decremental AP backpropagation reported here is similar to brain slice data from other pyramidal neurons, including neocortical layer 5 and CA1 hippocampal neurons (Stuart and Sakmann, 1994; Spruston et al., 1995; Magee and Johnston, 1997), although attenuation is slightly stronger in L2/3 than in L5 neurons; 300 μm from the soma AP amplitudes were 48 mV in L2/3 and 65 mV in L5 neurons (Larkum et al., 2001). There is also evidence for active AP backpropagation in L5 and hippocampal neurons in both the anesthetized and the awake rat, although the degree of dendritic AP attenuation may be sensitive to the behavioral state of the animal (Buzsáki et al., 1996; Buzsáki and Kandel, 1998; Kamondi et al., 1998; Quirk et al., 2001).

The decline in AP amplitude described here is less steep than reported previously for L2/3 pyramidal neurons *in vivo* (Svoboda et al., 1999). We found a comparably steep decline in amplitude only after blocking Na^+ channels with TTX. This discrepancy could be attributable to differences in somatic depths or locations of recordings in the dendritic tree, or both. The previous study included several dendritic recordings from higher-order branches, whereas our TTX experiments, demonstrating the dependence of AP backpropagation on Na^+ channels, were from the apical trunk. Another difference is that in the previous study sharp intracellular microelectrodes were used instead of patch pipettes. Partial block of the microelectrode tip, particularly in thin dendrites, might have resulted in underestimation of dendritic AP amplitudes. We encountered a similar problem with patch pipettes, in which AP amplitudes were reduced in high-access resistance recordings even at the soma. In addition, the single AP-evoked Ca^{2+} profile presented here (with a maximum at ~20% of the soma-pial distance) (Fig. 2) is comparable with previous *in vivo* measurements (Svoboda et al., 1997, 1999). The strong suppression of proximal dendritic Ca^{2+} transients by TTX *in vitro* demonstrates that these profiles can be explained only by activation of dendritic Na^+ channels (Fig. 3).

Distal dendritic Ca^{2+} influx

Single APs failed to evoke Ca^{2+} influx in the distal branches of the dendritic tuft. In contrast, brief high-frequency bursts of APs induced large distal Ca^{2+} transients even in subpial terminal branches both *in vitro* and *in vivo*. This demonstrates that Ca^{2+} channels are present throughout the apical dendritic tree. A single AP, although actively backpropagating, is probably too strongly attenuated along the apical dendrite to activate distal Ca^{2+} channels. From the Ca^{2+} profiles and the degree of AP attenuation, we estimate that this would occur when the AP amplitude dropped below ~50 mV. If it occurs in L2/3 neurons, a

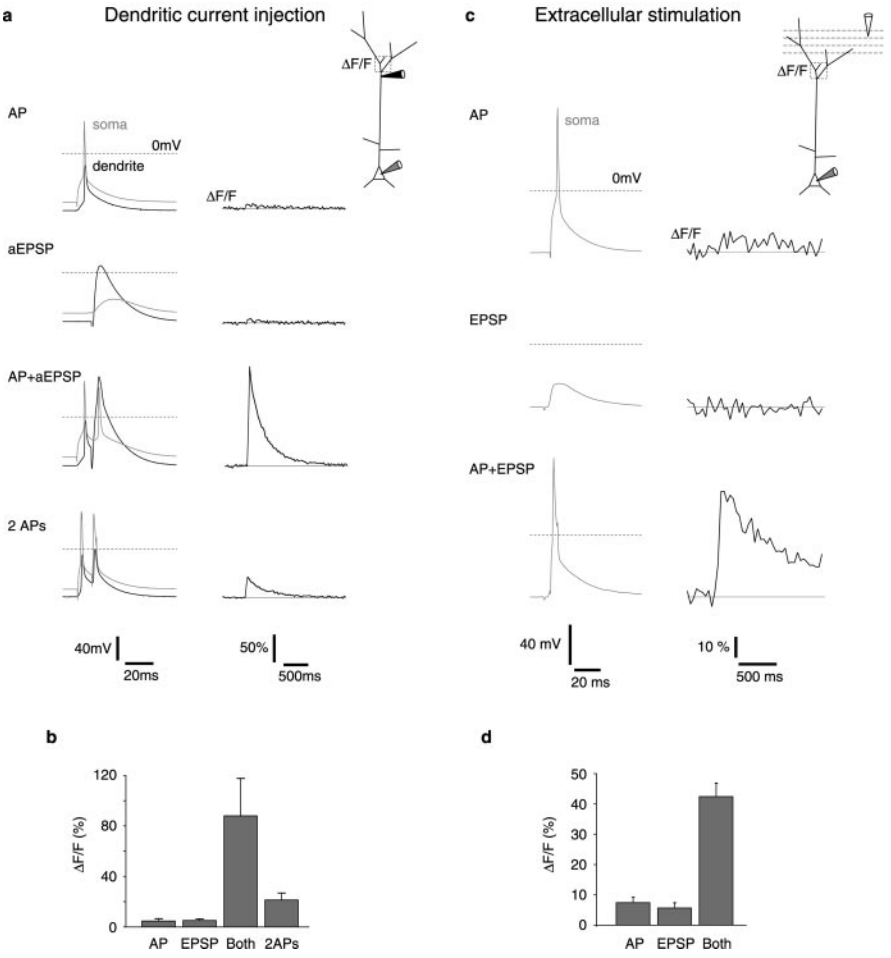

Figure 6. Pairing of AP and EPSP causes supralinear Ca^{2+} influx. *a*, Pairing of a backpropagating AP with an aEPSP. Simultaneous somatic and dendritic recordings from an L2/3 pyramidal neuron *in vitro*. Soma was 390 μm from pia. Dendritic recording was 160 μm from soma. Ca^{2+} transients were measured 220 μm from the soma, near the bifurcation. Left, Electrical recordings with the somatic traces in gray and the dendritic traces in black. Right, Ca^{2+} transients (means of 3 sweeps). Data are given for four stimulus protocols: single AP evoked by somatic current injection; aEPSP evoked by dendritic current injection (rise time constant 2 msec, decay time constant 8 msec); paired AP and aEPSP; two APs evoked by somatic current injections at 100 Hz. *b*, Summary data for five neurons, showing peak of Ca^{2+} transients measured near principal bifurcation during the different protocols. *c*, Voltage recordings from soma (left) and Ca^{2+} measurements from the dendrite (right; 175 μm from soma). Three stimulus protocols were used: a single AP, an EPSP, and both AP and EPSP. Extracellular stimulus and somatic current injection were delivered simultaneously so that the AP occurred before the peak of the EPSP. Somatic depth was 350 μm. Antagonists were included in the perfusing solution to partially block GABA receptors. *d*, Summary data for four neurons, showing peak of Ca^{2+} transients measured near the principal bifurcation during the different protocols.

change in calcium channel density and subtypes expressed along the dendrite could also contribute to the reduced calcium influx in the distal dendrite. During high-frequency bursts of APs, depolarization in the distal dendrite may summate so that the threshold for Ca^{2+} channel activation is reached. Ca^{2+} influx might even add a regenerative component to distal depolarization, similar to burst-evoked Na^{+}/Ca^{2+} APs reported in L5 pyramidal neurons (Larkum et al., 1999b; Helmchen et al., 1999). Broadening of later APs in a train was commonly observed with brief bursts of APs (Fig. 4*b*). Whether this reflects regenerative activity in the distal dendrite is unclear at present.

Comparison of *in vitro* and *in vivo* properties

A major conclusion of our study is that AP backpropagation and dendritic Ca^{2+} influx are comparable in cortical slices and the cortex of the anesthetized animal. This may be surprising at first glance because there is typically more background synaptic activity in the cortex of the anesthetized animal than in the cortical slice preparation (Paré et al., 1998). It is unclear, however, whether spontaneous input would necessarily result in a net suppression of backpropagation. In fact, EPSPs may boost AP backpropagation (Stuart and Häusser, 2001).

Furthermore, synaptic activity under anesthesia is not constant but varies between periods of little and more pronounced synaptic activity (commonly termed up and down states). This leads to membrane potential fluctuations on the time scale of hundreds of milliseconds, with periods of depolarization (10–20 mV up states) being driven by volleys of synaptic input. In our *in vivo* experiments we did not differentiate between data points obtained during up and down states. Our *in vivo* data are therefore derived from a mixture of up and down states; however, precise control of the number and frequency of action potentials generated *in vivo* was achieved more often during down than during up states. Hence more data points were typically gathered from the down state, which is prominent in the deeply anesthetized animal and represents a period of modest synaptic activity. Thus the current study establishes that biophysical properties of dendrites are comparable in brain slices and the living animal. This provides a framework from which to determine whether phenomena such as backpropagation and dendritic calcium influx are substantially different during periods of pronounced network activity, such as might be observed in the behaving animal.

There are indications from other cell types that active backpropagation is maintained in anesthetized and even awake animals. In apical dendrites of olfactory bulb mitral cells, backpropagation is nondecremental both *in vitro* and *in vivo*, despite the high levels of activity observed in the bulb under urethane anesthesia (Sobel and Tank, 1993; Bischofberger and Jonas, 1997; Chen et al., 1997; Charpak et al., 2001). Hence the effects of background synaptic activity on backpropagation under anesthesia *in vivo* are weak in both mitral cells and L2/3 pyramidal neurons. Background activity may be similarly ineffective in L5 and hippocampal neurons, in which extracellular recordings suggest that active backpropagation is maintained in awake behaving animals (Buzsáki and Kandel, 1998; Quirk et al., 2001).

Association of proximal and distal input

Another key finding of our study is that pairing a backpropagating AP with distal synaptic input results in a supralinear dendritic Ca^{2+} transient near the principal bifurcation. Large dendritic Ca^{2+} responses have also been observed in hippocampal and L5 neocortical pyramidal neurons, where they result from dendritic initiation of a regenerative Na^{+}/Ca^{2+} potential (Magee and

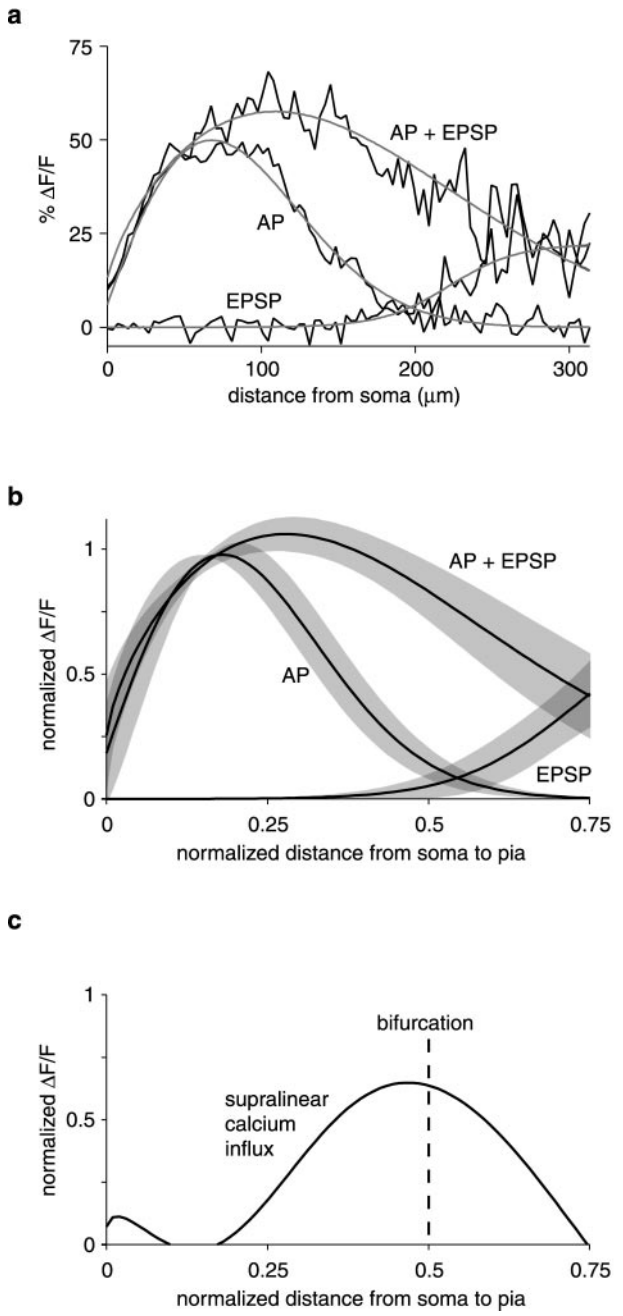

Figure 7. Distal extension of Ca^{2+} profiles after pairing. *a*, Low-magnification *in vitro* measurement of the spatial Ca^{2+} profiles in response to a single AP, to an extracellularly evoked distal EPSP, and to a combination of the two (same cell as in Fig. 4*d*; the bifurcation was 105 μm from the soma). Profiles were fitted with skewed Gaussian curves (AP, AP + EPSP) and a sigmoid curve (EPSP), respectively. The soma was 350 μm from the pia. The position of the bifucation is marked as a vertical dashed line. Antagonists were included in the perfusing solution to partially block GABA receptors. *b*, Normalized mean Ca^{2+} profiles for four neurons in response to AP, EPSP, and pairing of AP with EPSP. Each profile was normalized to the distance between soma and pia (range, 350–480 μm) and to the maximum value of the AP-evoked profile. Traces are the means of the fitted curves for four neurons. Shaded areas represent $\pm$ 1 SD from the mean. *c*, Supralinear Ca^{2+} influx that results from pairing AP and EPSP (difference between AP + EPSP and sum of AP and EPSP traces in *b*). The mean position of the bifucation is marked as a vertical dashed line.

Johnston, 1997; Schiller et al., 1997; Golding et al., 1999, 2002; Helmchen et al., 1999; Larkum et al., 1999a; Larkum and Zhu, 2002). Whether a dendritic Na^{+}/Ca^{2+} potential occurs in L2/3 dendrites is unclear, but the supralinear nature of the response suggests that a regenerative component is involved.

What is the functional significance of this distal dendritic excitation? Input to the distal dendrite includes feedback from higher-order cortical regions, some of which may carry state-dependent input such as attentional information (Cauller, 1995; Lamme et al., 1998). In addition, L2/3 neurons receive feedforward input via L4 neurons projecting predominantly to their proximal dendrites (Feldmeyer et al., 2002). The supralinear interaction of somatically evoked APs with distal EPSPs therefore provides a mechanism for the association of ascending sensory input and associative input to layer 1 by local cortical microcircuits. As in L5 neurons, coincident activity in these pathways facilitates distal dendritic Ca^{2+} influx, which will invade postsynaptic densities located in spines (Sabatini et al., 2002). This may be important for adjusting the strength of distal synapses (Golding et al., 2002). In summary, coincidence detection, as a mechanism to associate inputs in different cortical layers, is a feature common to neocortical pyramidal neurons.

References

Ahissar E, Sosnik R, Haidarliu S (2000) Transformation from temporal to rate coding in a somatosensory thalamocortical pathway. Nature 406:302–306.

Bischofberger J, Jonas P (1997) Action potential propagation into the presynaptic dendrites of rat mitral cells. J Physiol (Lond) 504:359–365.

Buzsáki G, Kandel A (1998) Somadendritic backpropagation of action potentials in cortical pyramidal cells of the awake rat. J Neurophysiol 79:1587–1591.

Buzsáki G, Penttonen M, Nádasdy Z, Bragin A (1996) Pattern and inhibition-dependent invasion of pyramidal cell dendrites by fast spikes in the hippocampus in vivo. Proc Natl Acad Sci USA 93:9921–9925.

Cauller L (1995) Layer I of primary sensory neocortex: where top-down converges after bottom-up. Behav Brain Res 71:163–170.

Cauller LJ, Connors BW (1994) Synaptic physiology of horizontal afferents to layer I in slices of rat SI neocortex. J Neurosci 14:751–762.

Cauller LJ, Kulics AT (1991) The neural basis of the behaviorally relevant N1 component of the somatosensory-evoked potential in SI cortex of awake monkeys: evidence that backward cortical projections signal conscious touch sensation. Exp Brain Res 84:607–619.

Chapin JK, Lin C-S (1990) The somatic sensory cortex of the rat. In: The cerebral cortex of the rat. (Kolb B, Tees RC, eds), pp 341–380. Cambridge, MA: MIT.

Charpak S, Mertz J, Beaurepaire E, Moreaux L, Delaney K (2001) Odor-evoked calcium signals in dendrites of rat mitral cells. Proc Natl Acad Sci USA 98:1230–1234.

Chen WR, Midtgaard J, Shepherd GM (1997) Forward and backward propagation of dendritic impulses and their synaptic control in mitral cells. Science 278:463–467.

Feldmeyer D, Lübke J, Silver RA, Sakmann B (2002) Synaptic connections between layer 4 spiny neurone–layer 2/3 pyramidal cell pairs in juvenile rat barrel cortex: physiology and anatomy of interlaminar signaling within a cortical column. J Physiol (Lond) 538:803–822.

Golding NL, Jung HY, Mickus T, Spruston N (1999) Dendritic calcium spike initiation and repolarization are controlled by distinct potassium channel subtypes in CA1 pyramidal neurons. J Neurosci 19:8789–8798.

Golding NL, Staff NP, Spruston N (2002) Dendritic spikes as a mechanism for cooperative long-term potentiation. Nature 418:326–331.

Golgi C (1886) Sur l'anatomie microscopique des organes centraux du système nerveux. Arch Ital Biol 7:15–47.

Häusser M, Spruston N, Stuart GJ (2000) Diversity and dynamics of dendritic signaling. Science 290:739–744.

Helmchen F (2000) Calibration of fluorescent calcium indicators. In: Imaging neurons, a laboratory manual (Yuste R, Lanni F, Konnerth A, eds), pp 32.1–32.9. Cold Spring Harbor, NY: Cold Spring Harbor Laboratory.

Helmchen F, Waters J (2002) Ca^{2+} imaging in the mammalian brain in vivo. Eur J Pharmacol 447:119–129.

Helmchen F, Svoboda K, Denk W, Tank DW (1999) *In vivo* dendritic calcium dynamics in deep-layer cortical pyramidal neurons. Nat Neurosci 2:989–996.

Kaiser KMM, Zilberter Y, Sakmann B (2001) Back-propagating action potentials mediate calcium signaling in dendrites of bitufted interneurons in layer 2/3 of rat somatosensory cortex. J Physiol (Lond) 535:17–31.

Kamondi A, Acsády L, Buzsáki G (1998) Dendritic spikes are enhanced by cooperative network activity in the intact hippocampus. J Neurosci 18:3919–3928.

Lamme VAF, Supèr H, Spekreijse H (1998) Feedforward, horizontal, and feedback processing in the visual cortex. Curr Opin Neurobiol 8:529–535.

Larkum ME, Zhu JJ (2002) Signaling of layer 1 and whisker-evoked Ca^{2+} and Na^{+} action potentials in distal and terminal dendrites of rat neocortical pyramidal neurons *in vitro* and *in vivo*. J Neurosci 22:6991–7005.

Larkum ME, Kaiser KM, Sakmann B (1999a) Calcium electrogenesis in distal apical dendrites of layer 5 pyramidal cells at a critical frequency of back-propagating action potentials. Proc Natl Acad Sci USA 96:14600–14604.

Larkum ME, Zhu JJ, Sakmann B (1999b) A new cellular mechanism for coupling inputs arriving at different cortical layers. Nature 398:338–341.

Larkum ME, Zhu JJ, Sakmann B (2001) Dendritic mechanisms underlying the coupling of the dendritic with the axonal action potential initiation zone of adult rat layer 5 pyramidal neurons. J Physiol (Lond) 533:447–466.

Lübke J, Egger V, Sakmann B, Feldmeyer D (2000) Columnar organization of dendrites and axons of single and synaptically coupled excitatory spiny neurons in layer 4 of the rat barrel cortex. J Neurosci 20:5300–5311.

Magee JC, Johnston D (1997) A synaptically controlled, associative signal for Hebbian plasticity in hippocampal neurons. Science 275:209–213.

Margrie TW, Brecht M, Sakmann B (2002) In vivo, low-resistance, whole-cell recordings from neurons in the anaesthetized and awake mammalian brain. Pflügers Arch 444:491–498.

Migliore M, Shepherd GM (2002) Emerging rules for the distributions of active dendritic conductances. Nat Rev Neurosci 3:362–370.

Mignard M, Malpeli JG (1991) Paths of information flow through the visual cortex. Science 251:1249–1251.

Paré D, Shink E, Gaudreau H, Destexhe A, Lang EJ (1998) Impact of spontaneous synaptic activity on the resting properties of cat neocortical pyramidal neurons in vivo. J Neurophysiol 79:1450–1460.

Quirk AC, Blum KI, Wilson MA (2001) Experience-dependent changes in extracellular spike amplitude may reflect regulation of dendritic action potential back-propagation in rat hippocampal pyramidal cells. J Neurosci 21:240–248.

Reyes A (2001) Influence of dendritic conductances on the input-output properties of neurons. Annu Rev Neurosci 24:653–675.

Sabatini BL, Oertner TG, Svoboda K (2002) The life cycle of Ca^{2+} ions in dendritic spines. Neuron 33:439–452.

Schiller J, Schiller Y, Stuart G, Sakmann B (1997) Calcium action potentials restricted to distal apical dendrites of rat neocortical pyramidal neurons. J Physiol (Lond) 505:605–616.

Sobel EC, Tank DW (1993) Timing of odor stimulation does not alter patterning of olfactory bulb unit activity in freely breathing rats. J Neurophysiol 69:1331–1337.

Spruston N, Schiller Y, Stuart G, Sakmann B (1995) Activity-dependent action potential invasion and calcium influx into hippocampal CA1 dendrites. Science 268:297–300.

Steriade M (2001a) Impact of network activities on neuronal properties in corticothalamic systems. J Neurophysiol 86:1–39.

Steriade M (2001b) Similar and contrasting results from studies in the intact and sliced brain. In: The intact and sliced brain, pp 134–142. Cambridge, MA: MIT.

Stuart GJ, Häusser M (2001) Dendritic coincidence detection of EPSPs and action potentials. Nat Neurosci 4:63–71.

Stuart GJ, Sakmann B (1994) Active propagation of somatic action potentials into neocortical pyramidal cell dendrites. Nature 367:69–72.

Svoboda K, Denk W, Kleinfeld D, Tank DW (1997) In vivo dendritic calcium dynamics in neocortical pyramidal neurons. Nature 385:161–165.

Svoboda K, Helmchen F, Denk W, Tank DW (1999) Spread of dendritic excitation in layer 2/3 pyramidal neurons in rat barrel cortex in vivo. Nat Neurosci 2:65–73.

Tsubokawa H, Ross WN (1996) IPSPs modulate spike backpropagation and associated $[Ca^{2+}]_i$ changes in the dendrites of hippocampal CA1 pyramidal neurons. J Neurophysiol 76:2896–2906.

Vetter P, Roth A, Häusser M (2001) Propagation of action potentials in dendrites depends on dendritic morphology. J Neurophysiol 85:926–937.

Yuste R, Tank DW (1996) Dendritic integration in mammalian neurons, a century after Cajal. Neuron 16:701–716.

Zilles K (1990) Anatomy of the neocortex: cytoarchitecture and myeloarchitecture. In: The cerebral cortex of the rat (Kolb B, Tees RC, eds), pp 77–113. Cambridge, MA: MIT.